Nanotechnology

DOI: 10.1002/ange.200502128

Fabrication of Random Assemblies of Metal Nanobands: A General Method**

*Michael E. Hyde, Trevor J. Davies, and Richard G. Compton**

Nanoscale electrodes have several advantages over their macroscopic counterparts: they are well suited to applications that require high sweep rates, low internal-resistance (iR) drops, and low capacitance.[1] A significant disadvantage of such electrodes is, however, that they generate extremely small currents. One useful compromise is to use a band electrode, in which the electrode is small enough in one dimension to give rise to nonlinear diffusion, while its size in the other dimension is increased to maximize the current output. Band electrodes are particularly favored when attempts are made to achieve very low analytical detection limits: the part of the residual current associated with the double-layer charging is lowered in proportion to the surface area of the electrode, while the Faradaic current is not.[2]

Nanoband electrodes are usually fabricated by using one of two general methods. The simpler of these approaches is to generate an insulator-metal-insulator sandwich and then expose one of the edges by polishing or cutting the material. If vacuum-evaporated films are used, extremely narrow bands (potentially down to approximately 1 nm) may be created. However, the technique suffers from some difficulties: the band width is defined by the thickness of the deposited film, which may be difficult to determine accurately. In addition, polishing of such small electrodes is likely to cause significant variations in its final shape, surface area, and so forth. There may be significant doubts about the real surface area of the band even when no polishing step is used.[3] This method is best suited to the creation of single bands.

The other commonly used method involves the use of lithography. In this case, there are two possibilities: First, a metal film may be evaporated on to a substrate, photoresist is applied and patterned lithographically, the unprotected metal is etched, and finally the remaining photoresist is removed.[4] Second, a "lift-off" technique may be employed, in which the photoresist is applied directly to the substrate and patterned.

[*] M. E. Hyde, T. J. Davies, Prof. R. G. Compton
Physical and Theoretical Chemistry Laboratory
Oxford University
South Parks Road, Oxford OX1 3QZ (UK)
Fax: (+44) 1865-275-410
E-mail: richard.compton@chemistry.ox.ac.uk

[**] The authors thank the EPSRC for studentships for T.J.D. and M.E.H. We further thank Roger Bowler for his expertise in the preparation of the highly ordered pyrolytic-graphite (HOPG) electrode housing, Robert M. J. Jacobs for his help with the metal deposition, and Andrew J. Wain for his assistance with the sodium sulfite experiments. T.J.D. thanks Lincoln College and the Lord Crewe's Society for a scholarship (2004–2005) and Abi Smith for all her support.

© 2005 Wiley-VCH Verlag GmbH & Co. KGaA, Weinheim

The metal film is then applied on top, and when the remaining photoresist is removed, the corresponding metal film is also removed, thus leaving only the metal attached directly to the substrate.[4] These methods are highly reproducible and allow precise control of the electrode geometry. Recently, band widths and gap widths down to 30 nm have been achieved by using a lift-off procedure combined with high-resolution electron-beam lithography.[5] Lithographic methods, however, require specialized equipment and are relatively complex to implement.

A related approach to the modification of surfaces with conductive bands has been explored by Penner and co-workers,[6–8] who have shown that metal nanowires may be obtained by selective electrodeposition of conducting metal oxides onto the step edges present at highly ordered pyrolytic-graphite (HOPG) surfaces, followed by reduction with hydrogen. (Although the direct deposition of metals onto the step edges is possible and conceptually simpler, the resulting wires are usually of poorer quality for various reasons.[6]) This effect results from the specialized structure of HOPG, which consists of atomically flat basal-plane graphite terraces separated by defects that expose relatively thin (335 pm or multiples thereof) bands of edge-plane graphite. Given the correct deposition potential, these edges are strongly favored because of their much greater electrochemical activity.[9–11]

We have recently extended this methodology in a three-step electrochemical process to generate nanotrenches by using the following procedure:[9] MoO_2 nanowires are deposited on HOPG in a manner similar to that described by Penner and co-workers. A reducing potential is then applied to a solution of 4-nitrobenzenediazonium ions, thus leading to the deposition of a polymeric film on the electrode which has a thickness on the order of 10 nm. (Although the molybdenum oxide deposited under these conditions is in fact a mixture of MoO_2 and MoO_3, it is usually described as MoO_2.[6–9] Herein, we follow this convention to avoid confusion.) Finally, the MoO_2 is dissolved in hydrochloric acid; as with the lithographic "lift-off" procedure, any polymer above the MoO_2 wires is removed at the same time. The result is that the HOPG electrode is covered entirely by an impermeable film except for the step edges, which are uncovered. Herein, we extend this method further through the presentation of a simple, general, and mostly solution-phase method for the generation of assemblies of metal nanobands by using the original MoO_2 nanowires as a template.

The process for the fabrication of these nanoband assemblies is illustrated conceptually in Figure 1. MoO_2 nanowires were electrodeposited onto the freshly cleaved HOPG surface (Figure 1a) using a solution of 1.1 mM sodium molybdate, 1M sodium chloride, and 1M ammonium hydroxide adjusted to pH 8.5 with sodium hydroxide. The mean thickness of the nanowires has been shown to be dependent on the deposition time, thus allowing wires with controlled diameters to be prepared (see below). In the present case, deposition was performed at −1.0 V (versus the saturated calomel electrode (SCE)) for 130 seconds (Figure 1b). An atomic force microscopy (AFM) image of the resulting

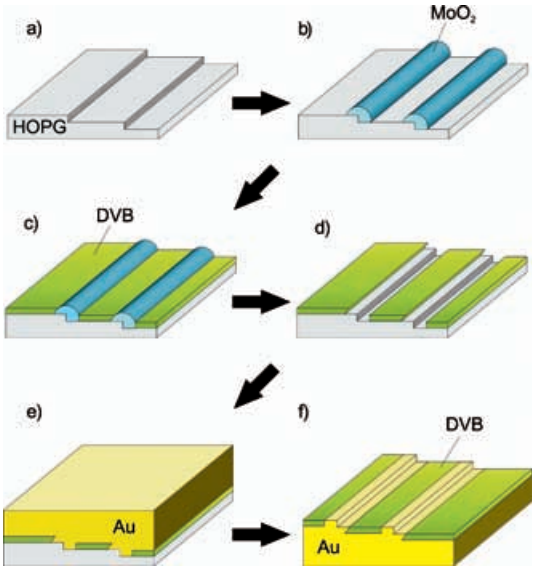

Figure 1. Schematic diagram showing the six stages involved in metal-nanoband fabrication: a) freshly cleaved HOPG; b) after deposition of the MoO_2 nanowires; c) after deposition of the DVB (divinylbenzene) polymer film, d) after removal of the MoO_2 nanowires; e) after evaporation of a gold layer onto the surface; and f) after cleavage of the gold layer from the HOPG substrate.

nanowires is shown in Figure 2a. To test the homogeneity of the nanowire coverage, AFM images were collected at several separated points on the electrode; this image (and those presented below) was found to be representative of the whole electrode.

The second step was to cover the remaining exposed carbon again with a layer of polymer. However, a solution of 50 mM divinylbenzene (DVB) and 0.1M tetrabutylammonium perchlorate in acetonitrile was used instead of the solution of 4-nitrobenzenediazonium. DVB has been shown to readily polymerize under oxidation conditions,[12] and we found that

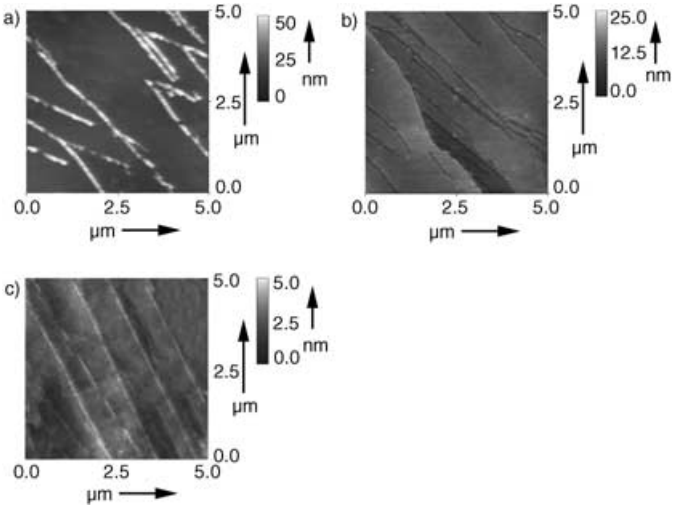

Figure 2. AFM images showing steps in nanoband fabrication: a) MoO_2 nanowires (corresponding to Figure 1b); b) nanotrenches (corresponding to Figure 1d); and c) completed gold nanobands (corresponding to Figure 1f).

© 2005 Wiley-VCH Verlag GmbH & Co. KGaA, Weinheim

application of +1.6 V for 30 s reproducibly generated an even, relatively insulating film (see below), with a thickness of approximately 5–10 nm (Figure 1c).

The nanowires were removed and nanotrenches created by immersion of the HOPG electrode in a stirred solution of 1M hydrochloric acid for 300 s (Figure 1d). An AFM image of these nanotrenches is shown in Figure 2b. The texture of the DVB film is clearly visible when compared with the background HOPG in Figure 1a, and the nanotrenches have a mean depth of approximately 6 nm. It should be noted that the fact that the MoO_2 deposits can be removed in this way implies that the film is somewhat porous, thus allowing the solution of HCl to penetrate. However, the surface is effectively blocked in an electrochemical sense: cyclic voltammetry (CV) in a solution of 1.0 mM $[Ru(NH_3)_6]^{3+}$/1M KCl after DVB-film deposition shows a tiny signal (in proportion to the results obtained from a bare HOPG electrode or metal nanobands). This residual current presumably arises from the slightly porous nature of the film, but is negligible relative to the contribution from the completed nanoband array. The effect of a polymer blocking HOPG electrodes has been previously discussed in greater detail.[9]

The electrode was removed from the acid, rinsed, and dried. A 200-nm-thick layer of gold was then evaporated on top of the nanotrenches under the conditions described in the Experimental Section, and a supporting stub was attached to the gold layer using a cyanoacrylate adhesive (Figure 1e). The HOPG was finally cleaved as close to the gold layer as possible using a knife. The original HOPG block is regenerated, and any thin layer of HOPG that remains on top of the gold layer may be removed with adhesive tape, thus leaving what was originally the underside of the gold layer exposed. We found that the DVB layer adheres preferentially to the gold surface (rather than the HOPG block) and leaves the structure illustrated in Figure 1f, which has exposed gold nanobands surrounded by an insulating layer of polymer. (AFM analysis of the HOPG surface separated from the gold layer showed no sign of nanotrenches, thus confirming that the polymerized DVB deposit adheres to the gold surface.) An AFM image of these bands is shown in Figure 2c. Note that the decreasing height scale in Figure 2a–c shows that the nanobands are somewhat difficult to resolve because of the very small height difference between the DVB layer and the exposed gold surface. This small height difference might be predicted from Figure 1f, as the edges of the bands should in theory be flush with the top of the DVB layer.

To study the nanobands in more detail, a representative band was chosen and examined at a scan range of approximately 800 nm. An AFM image of this band is shown in Figure 3a, along with a section analysis of a line perpendicular to the nanoband axis in Figure 3c. Some important features are apparent: the width of the nanoband is around 180 nm, the maximum height of the nanoband above the polymer layer is approximately 700 pm, and the band has a characteristic "m" shape. The depth of the central "v" is approximately 300 pm, suggesting that this shape is related to that of the original HOPG step edge. The shape of the band may in fact be beneficial in terms of the electrochemical behavior of the electrode, as most of the current flow at a nanoband electrode occurs near the edges. Therefore, a partial reinforcement of the metal thickness at the band edges may decrease the ohmic drop of the nanoband precisely where this drop is required. Next, the sample was analyzed by using scanning tunnel microscopy (STM). Initially, the scan-feedback parameters were increased as much as possible ("constant-current" mode). On typical surfaces (in which the conductivity is uniform), this procedure gives the most accurate reproduction of the real surface. However, we found that in the current case although the texture of the background and the band itself are well resolved, the height of the band is significantly overreported (Figure 3c). In addition, the STM current appears as in Figure 3d when the feedback parameters are minimized ("constant-height" mode). Together these observations are direct evidence of the presence and relatively much lower conductivity of the DVB film. In constant-height mode, the bias is set high enough for electrons to tunnel through the DVB film. When the tip reaches a nanoband, the much higher conductivity of the gold surface causes the tip to overcompensate, thus moving a large distance away to maintain the same current. For this reason, the absolute heights recorded in the constant-current STM mode should be considered unreliable and have been omitted from the relevant figures. In constant-height mode, the tip remains at a fixed height (irrespective of any surface features) and the tunneling current is recorded. We would clearly expect the gold areas to pass a much greater current at a given bias potential, which is exactly as observed.

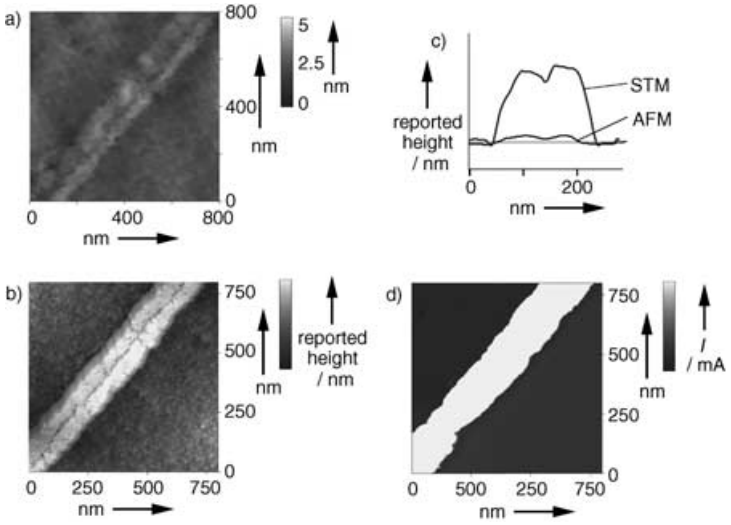

Figure 3. A single gold nanoband shown at a scan range of approximately 800 nm. a) AFM image (height). b) Constant-current STM image (height). c) Section analyses perpendicular to the band axis from the AFM (a) and constant-current STM (b) images; note that the actual height of the band is approximately 0.8 nm (estimated by using AFM). d) Constant-height STM image (current).

In principle, the method described above for the generation of nanobands should be effective for any material that can be evaporated onto the nanotrenches. To test this hypothesis, the procedure was repeated exactly as described above except silver was used instead of gold in the evaporation step. It was found that the resulting nanobands were

 © 2005 Wiley-VCH Verlag GmbH & Co. KGaA, Weinheim

impossible to resolve by AFM because of the small height of the bands relative to the roughness of the surface. Again, however, the bands are clearly visible when constant-current STM is used. STM images at two scan ranges are shown in Figure 4. Again, the "m" shape is visible, and the bands shown

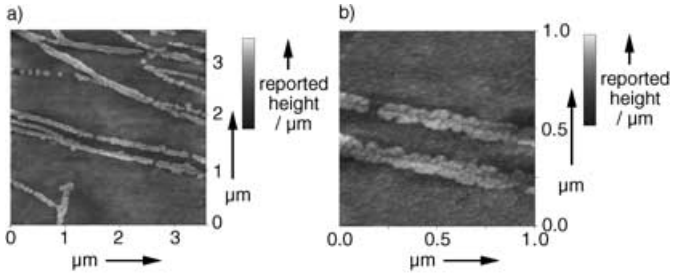

Figure 4. Constant-current STM images of silver nanobands at various scan ranges: a) $3\times3\ \mu m^2$ and b) $1\times1\ \mu m^2$.

in Figure 4b have a width of approximately 150 nm, which is consistent with the results for the gold nanobands (given that some variation in nanowire/nanotrench width over the whole electrode is always observed).

As stated above, it should also be possible to control the mean nanoband width by adjusting the length of time for which MoO_2 is deposited, which was tested by repeating the above procedure. However, this time MoO_2 was deposited at -1.0 V for 30 s (see Figure 5a). Finer nanowires were produced with a mean diameter of approximately 80–90 nm, nanotrenches were produced as usual from these wires, and copper was evaporated onto the surface to a depth of 200 nm. After cleavage, again no nanobands could be distinguished by using AFM, but STM clearly revealed their presence (Figure 5b,c). As expected, the bands are narrower than in the two previous cases: the magnified image in Figure 5c shows a typical band with a width of 100 nm.

The nanoband arrays produced by using this method were analyzed voltammetrically. An important parameter for any

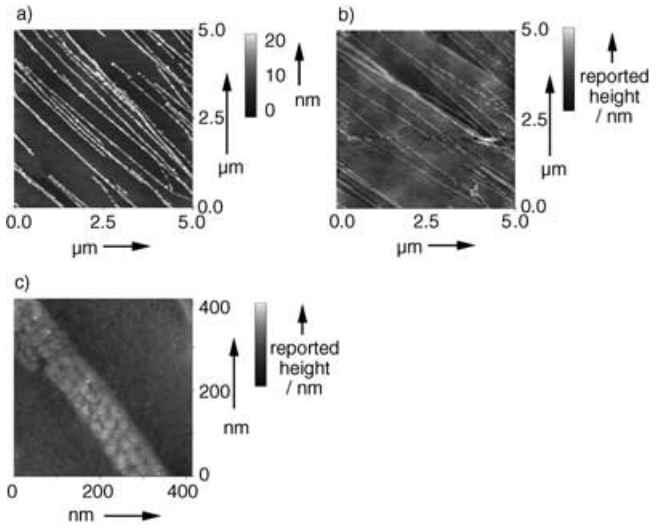

Figure 5. a) AFM image of MoO_2 nanowires after deposition for 30 s. b), c) Constant-current STM images of copper nanobands prepared using the nanowires in (a).

type of electrode array is the global coverage Θ as defined by Equation (1):

$$\Theta = \frac{A_{ins}}{A_{array}} \tag{1}$$

A_{ins} is the area of insulating material and A_{array} is the total surface area of the array. It follows that the area of electrode material is given by $A_{array}(1-\Theta)$. Now consider the case in which we perform cyclic voltammetry at an electrode of material i in a simple one-electron redox couple given by Equation (2):

$$A + e \underset{}{\overset{k^o,\alpha}{\rightleftharpoons}} B \tag{2}$$

A and B are the oxidized and reduced species, respectively, k^o is the electron-transfer rate constant, and α is the symmetry coefficient for the heterogeneous reaction to give B. The observed response is dependent on a number of system parameters, such as the diffusion coefficient D, the area of the electrode A_{elec}, and k^o. For the purpose of this argument, we label the whole response as $[I-E(k^o)]$. Now consider the case in which we have a nanoband array of material i and global coverage Θ in the same redox couple and $A_{array}=A_{elec}$. Previous investigations have shown that if the spacing between the individual bands is considerably smaller than the diffusion-layer thickness δ, the CV response will be given by $[I-E\{k^o(1-\Theta)\}]$.[10,13] That is, the I–E response of the array will be equal to that of a naked electrode of the same area in the same redox couple but with an electron-transfer rate constant of $k^o(1-\Theta)$.

Figure 6a illustrates a cyclic voltammogram recorded with the gold nanoband array in Figure 2c immersed in a solution of 1.0 mM $[Ru(NH_3)_6]^{3+}$/1M KCl, in which the scan rate was $1\ V s^{-1}$. Overlaid as a dashed curve is the corresponding response for a gold electrode of the same surface area, that is, $A_{elec}=A_{array}$ (in this case the gold electrode was prepared by gold plating a metal slab and was used in the same electrode housing as the array). It is necessary to estimate the proportion of the array surface which is exposed gold to compare these curves meaningfully. To this end, ten STM images, each with a scan range of 5 μm, were collected from randomly selected points on the electrode surface. A custom-written Matlab program was then used to analyze the images by using the following method: the bands appear significantly higher on the surface than the DVB background so the band surface and DVB surface can be differentiated simply by setting an appropriate height threshold and counting the total number of data points above and below this threshold for all the images. In this way, the proportional area of exposed gold was found to be approximately 10%. Although the polymer coverage of the nanoband array was approximately 90%, an I–E response almost equal in magnitude to that of the "naked" gold electrode was observed.

In addition, the peak-to-peak separation for the array was larger than that for the naked electrode. This observation is in complete agreement with the theory discussed above. At $1\ V s^{-1}$, the diffusion-layer thickness at the peak potential of the forward scan will be approximately 15 μm.[14] It can be seen from Figure 2c that the spacing between the bands is less

 © 2005 Wiley-VCH Verlag GmbH & Co. KGaA, Weinheim

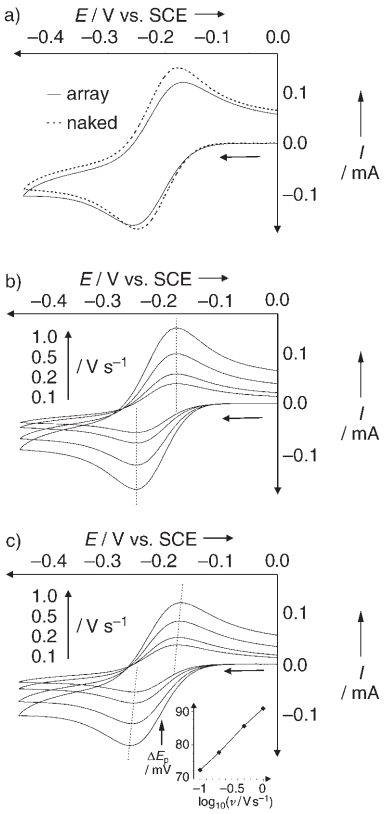

Figure 6. a) Cyclic voltammogram taken at 1 $V s^{-1}$ in a solution of 1.0 mM $[Ru(NH_3)_6]^{3+}$/1 M KCl at the gold nanoband array in Figure 2c (solid) and a gold electrode of the same surface area (dashed). b), c) Cyclic voltammograms taken at varying scan rates in a solution of 1.0 mM $[Ru(NH_3)_6]^{3+}$/1 M KCl at the gold electrode (b) and the gold nanoband array (c).

than 1 μm; therefore, the observed response obtained in Figure 6 is as expected. The fact that the nanoband array with a coverage Θ of approximately 0.9 gives a response almost equal in magnitude to that of the naked electrode indicates that the mass transport to the nanobands must be considerably faster than to the naked electrode. A potential application of this response is illustrated in Figure 6b,c, which shows cyclic voltammograms recorded at various scan rates at the naked gold electrode and the gold nanoband array in the same solution used for the cyclic voltammogram shown in Figure 6a. The $[Ru(NH_3)_6]^{3+}/[Ru(NH_3)_6]^{2+}$ redox reaction has an electron-transfer rate constant of approximately 0.5 $cm s^{-1}$ at the gold electrodes, thus making it electrochemically reversible at the scan rates employed in Figure 6b.[15,16] Hence, the same peak-to-peak separation ΔE_p (≈ 60 mV) in Figure 6b was observed at all scan rates. In this situation, only thermodynamic data for the redox reaction can be deduced and much higher scan rates would be needed (or smaller electrodes) to deduce reliable kinetic data.[15,16] However, the nanoband array effectively reduces k^o to $(1-\Theta)k^o$, such that the redox reaction now appears to be quasireversible at the scan rates employed, as shown in Figure 6c, in which ΔE_p increases with scan rate. Thus, well-characterized nanoband arrays could have fundamental applications (namely, alternative methods to investigate fast electron-transfer reactions) in addition to their use in electroanalysis. Also, as well as scanning probe microscopy (SPM) image analysis, a nanoband array could be characterized by using a redox couple of known k^o (for example, determined through a previous microdisk experiment). Subsequent analysis of the nanoband cyclic voltammograms would yield k^o_{eff}, in which $(1-\Theta) = k^o_{eff}/k^o$.

In conclusion, we have demonstrated a method for the generation of large assemblies of metal nanobands (the size of which was only limited by the HOPG block employed). The method has been shown to be effective for the generation of gold, silver, and copper nanobands and may work with any material that can be evaporated onto the electrode surface to form a stable 200-nm-thick layer. Control of the mean nanoband width has also been demonstrated: we have created bands with widths between approximately 90 and 180 nm by varying the deposition time of MoO_2. In principle, the method can be readily extended to produce narrower bands simply by decreasing the deposition time further. However, in practice we found this approach somewhat problematic as shorter deposition times tended to produce "patchier" and less-continuous nanowires. Conversely, wider nanobands can be produced by increasing the deposition time. Although not considered in the present study, it should also be possible to vary the nanoband density. The band density is a function of the density of the step edges on the HOPG surface; it could, therefore, be decreased by employing a higher grade of HOPG or increased by using a lower grade.[17] The method for the preparation of a fresh HOPG surface can also effect the edge-step density; for example, McDermott and McCreery found that cleavage of an HOPG surface with a sharp blade results in far less edge steps than the adhesive cleaving technique employed herein.[18]

Experimental Section

All reagents were of the highest grade that was commercially available and were used as received without any further purification. These were sodium molybdate (Aldrich; 98 + %), potassium chloride (Reidel-de-Haen; ≥ 99.5%), sodium chloride (BDH; AnalaR), ammonium chloride (BDH, GPR), sodium hydroxide (Acros; ≥ 98%), hexaammineruthenium(III) chloride (Aldrich; 98%), sulfuric acid (BDH; AnalaR, sp. gr. 1.84), sodium sulfide (Aldrich; 98 + %), tetrabutylammonium perchlorate (Fluka; puriss electrochemical grade), and DVB (Aldrich; 80%, mixture of isomers). All aqueous solutions were prepared with deionized water with a resistivity of not less than 18.2 MW cm (Vivendi water systems, UK). Solutions of DVB were prepared with acetonitrile (Fischer Scientific; anhydrous synthesis grade). The temperature was 294 ± 2 K for all experiments.

The metal layers were prepared on the HOPG surface by metal-vapor deposition in a BOC Edwards Auto 306 vacuum coater with a Cryo-pumping system (with a base pressure of 2×10^{-7} mbar). The metals were evaporated from an alumina-coated molybdenum boat (R. D. Mathis, Long Beach, CA, USA) with a 3.2-V 300-A power supply. The current was controlled so that the rate of deposition on the sample was maintained at about 1 $nm s^{-1}$ and monitored with a quartz-crystal microbalance (FTM5 thickness monitor, BOC Edwards), which was mounted adjacent to the sample, both of which were 120 mm from the evaporation source. During the evaporation, the sample was rotated at about 5 rpm around a circle radius of 50 mm centered directly above the source with the pressure maintained below 1×10^{-6} mbar. The evaporation was stopped once the film had reached the required thickness, and the system was

 © 2005 Wiley-VCH Verlag GmbH & Co. KGaA, Weinheim

allowed to cool to room temperature before venting and removing the sample. Gold and silver were obtained from Alfa (99.99%), and copper was obtained from Goodfellow (99.999%).

Voltammetric measurements were carried out with a μ-Autolab type II potentiostat (ECO-Chemie, The Netherlands). All electrochemical experiments were conducted by using a three-electrode configuration, in which the substrate for the working electrode was basal-plane HOPG. The HOPG was purchased in the form of a $10 \times 10 \times 2\ mm^3$ block from SPI Supplies (PA, USA; type SPI-2). The HOPG experiments were conducted by using the HOPG housing, as previously described, which resulted in an exposed electrode area of $0.32\ cm^2$.[19] The HOPG surfaces were prepared by cleavage with adhesive tape before each experiment. At all times, the counter electrode was a bright platinum wire with a surface area much larger than that of the working electrode. A saturated calomel electrode (Radiometer, Copenhagen, Denmark) was employed as the reference.

All the SPM experiments employed a Multimode SPM (Digital Instruments, now a division of Veeco). A model "J" scanner was used, with a lateral range of $125 \times 125\ \mu m$ and a vertical range of $5\ \mu m$. All the AFM experiments were performed in the tapping mode, with standard silicon probes (Nascatec GMBH part NST-NCHF). STM experiments used Pt/Ir tips (Veeco part PT) at a bias of $+200$ mV in all experiments. All SPM experiments were performed in air.

Received: June 19, 2005
Published online: September 20, 2005

Keywords: electrochemistry · nanostructures · scanning probe microscopy · surface chemistry

[1] M. Samuelsson, M. Armgarth, C. Nylander, *Anal. Chem.* **1991**, *63*, 931.
[2] J. Wang, X. Rongrong, T. Baomin, J. Wang, C. L. Renschler, C. A. White, *Anal. Chim. Acta* **1994**, *293*, 43.
[3] S. L. Caston, R. L. McCarley, *J. Electroanal. Chem.* **2002**, *529*, 124.
[4] R. W. Dyson, *Specialty Polymers*, Chapman and Hall, New York, **1987**.
[5] K. Ueno, M. Hayashida, J.-Y. Ye, H. Misawa, *Electrochem. Commun.* **2005**, *7*, 161.
[6] E. C. Walter, M. P. Zach, F. Favier, B. J. Murray, K. Inazu, J. C. Hemminger, R. M. Penner, *ChemPhysChem* **2003**, *4*, 131.
[7] M. P. Zach, K. Inazu, K. H. Ng, J. C. Hemminger, R. M. Penner, *Chem. Mater.* **2002**, *14*, 3206.
[8] M. P. Zach, K. H. Ng, R. M. Penner, *Science* **2000**, *290*, 2120.
[9] T. J. Davies, M. E. Hyde, R. G. Compton, *Angew. Chem.* **2005**, *117*, 5251; *Angew. Chem. Int. Ed.* **2005**, *44*, 5121.
[10] T. J. Davies, R. R. Moore, C. E. Banks, R. G. Compton, *J. Electroanal. Chem.* **2004**, *574*, 123.
[11] C. E. Banks, T. J. Davies, G. G. Wildgoose, R. G. Compton, *Chem. Commun.* **2005**, 829.
[12] H. O. Finklea, R. S. Vithanage, *J. Electroanal. Chem.* **1984**, *161*, 283.
[13] C. Amatore, J. M. Saveant, D. Tessier, *J. Electroanal. Chem.* **1983**, *147*, 39.
[14] T. J. Davies, E. R. Lowe, S. J. Wilkins, R. G. Compton, *ChemPhysChem* **2005**, *6*, 1340.
[15] H. Matsuda, Y. Ayabe, *Z. Elektrochem. Angew. Phys. Chem.* **1955**, *59*, 494.
[16] H. Matsuda, Y. Ayabe, *Z. Elektrochem. Angew. Phys. Chem.* **1955**, *59*, 1059.
[17] https://secure.2spi.com/catalog/new/hopgsub.shtml.
[18] M. T. McDermott, R. L. McCreery, *Langmuir* **1994**, *10*, 4307.
[19] R. Bowler, T. J. Davies, M. E. Hyde, R. G. Compton, *Anal. Chem.* **2005**, *77*, 1916.

 © 2005 Wiley-VCH Verlag GmbH & Co. KGaA, Weinheim